

Intracoronary Imaging, Cholesterol Efflux, and Transcriptomes After Intensive Statin Treatment



The YELLOW II Study

Annapoorna S. Kini, MD,^a Yuliya Vengrenyuk, PhD,^a Khader Shameer, PhD,^b Akiko Maehara, MD,^c Meerarani Purushothaman, PhD,^a Takahiro Yoshimura, MD,^a Mitsuaki Matsumura, BS,^c Melissa Aquino, MS,^a Nezam Haider, PhD,^a Kipp W. Johnson, BS,^b Ben Readhead, MBBS,^b Brian A. Kidd, PhD,^b Jonathan E. Feig, MD, PhD,^a Prakash Krishnan, MD,^a Joseph Sweeny, MD,^a Mahajan Milind, PhD,^a Pedro Moreno, MD,^a Roxana Mehran, MD,^a Jason C. Kovacic, MD, PhD,^a Usman Baber, MD,^a Joel T. Dudley, PhD,^b Jagat Narula, MD, PhD,^a Samin Sharma, MD^a

ABSTRACT

BACKGROUND Despite extensive evidence demonstrating the beneficial effects of statins on clinical outcomes, the mechanisms underlying these effects remain elusive.

OBJECTIVES This study assessed changes in plaque morphology using intravascular imaging, with a comprehensive evaluation of cholesterol efflux capacity (CEC) and peripheral blood mononuclear cell (PBMC) transcriptomics in patients receiving high-dose statin therapy.

METHODS In a prospective study, 85 patients with stable coronary artery disease underwent percutaneous coronary intervention for a culprit lesion, followed by intracoronary multimodality imaging, including optical coherence tomography (OCT) of an obstructive nonculprit lesion. All subjects received 40 mg of rosuvastatin daily for 8 to 12 weeks, when the nonculprit lesion was reimaged and intervention performed. Blood samples were drawn at both times to assess CEC and transcriptomic profile in PBMC.

RESULTS Baseline OCT minimal fibrous cap thickness (FCT) was $100.9 \pm 41.7 \mu\text{m}$, which increased to $108.6 \pm 39.6 \mu\text{m}$ at follow-up, and baseline CEC was 0.81 ± 0.14 , which increased at follow-up to 0.84 ± 0.14 ($p = 0.003$). Thin-cap fibroatheroma prevalence decreased from 20.0% to 7.1% ($p = 0.003$). Changes in FCT were independently associated with CEC increase by multivariate analysis (β : 0.30; $p = 0.01$). PBMC microarray analysis detected 117 genes that were differentially expressed at follow-up compared to baseline, including genes playing key roles in cholesterol synthesis (*SQLE*), regulation of fatty acids unsaturation (*FADS1*), cellular cholesterol uptake (*LDLR*), efflux (*ABCA1* and *ABCG1*), and inflammation (*DHCR24*). Weighted coexpression network analysis revealed unique clusters of genes associated with favorable FCT and CEC changes.

CONCLUSIONS The study demonstrated an independent association between fibrous cap thickening and improved CEC that may contribute to morphological changes suggesting plaque stabilization among patients taking intensive statin therapy. Furthermore, the significant perturbations in PBMC transcriptome may help determine the beneficial effects of statin on plaque stabilization. (Reduction in Coronary Yellow Plaque, Lipids and Vascular Inflammation by Aggressive Lipid Lowering [YELLOW II]; [NCT01837823](https://doi.org/10.1016/j.jacc.2016.10.029)) (J Am Coll Cardiol 2017;69:628-40) © 2017 by the American College of Cardiology Foundation.



Listen to this manuscript's audio summary by JACC Editor-in-Chief Dr. Valentin Fuster.



From the ^aDivision of Cardiology, Mount Sinai Hospital and Icahn School of Medicine at Mount Sinai, New York, New York; ^bIcahn Institute for Genomics and Multiscale Biology, Icahn School of Medicine at Mount Sinai, New York, New York; and the ^cDivision of Cardiology, Columbia University Medical Center and Cardiovascular Research Foundation, New York, New York. Supported by AstraZeneca Investigator-Sponsored Study Program, InfraRedx, and Mount Sinai catheterization laboratory endowment funds to Dr. Kini. Dr. Maehara has received research grants from and serves as a consultant to Boston Scientific and St. Jude Medical. Dr. Moreno is a speaker for St. Jude Medical, AstraZeneca, and Abbott; is co-founder of InfraRedx, Inc; and holds equity in InfraRedx and patent rights to LipiScan NIR coronary imaging system. Dr. Kovacic has received support from

Clinical benefits of lowering lipids by using statins in primary and secondary prevention of cardiovascular disease have been established by several landmark randomized clinical studies (1-4). Subsequent studies provided strong evidence for statins improving clinical outcomes through suppression of inflammation and other lipid-lowering independent properties (5,6). Beyond lipid lowering, the pleiotropic effects of statins also contribute to favorable changes in plaque biology, documented by multiple imaging studies. Statin therapy has demonstrated a substantial reduction in atheroma volume by intravascular ultrasonography (IVUS) (7,8), plaque lipid content by near infrared spectroscopy (NIRS) (9), percentage of necrotic core area by virtual histology (10), and increase in fibrous cap thickness (FCT) assessed by optical coherence tomography (OCT) (11,12). Additionally, more intensive statin therapy leads to more favorable change in plaque morphology (8,9). Despite the extensive evidence for statins' beneficial effects on plaque size and morphology, the mechanisms underlying these effects in humans remain incompletely understood.

SEE PAGE 641

Decreased levels of high-density lipoprotein cholesterol (HDL-C) have been associated with increased cardiovascular risk in numerous epidemiological studies; however, randomized controlled trials with pharmacological intervention raising HDL-C have failed to reduce cardiovascular disease events (13,14). High-density lipoprotein promotes several atheroprotective functions including reverse cholesterol transport, the pathway by which HDL accepts peripheral cholesterol and delivers it to the liver for excretion (15). Macrophage-specific cholesterol efflux to lipid-deficient apolipoprotein AI (apo A-I) particles binding to the ATP-binding cassette A1 transporter (ABCA1) is considered the most relevant to atherosclerosis (16). Cholesterol efflux capacity (CEC) has demonstrated an inverse relationship with incidence of cardiovascular events in population-based studies (16,17) and has been shown to improve cardiovascular disease risk prediction beyond conventional risk factors (18).

Whether statins can improve HDL function and decrease low-density lipoprotein cholesterol (LDL-C) is controversial. Results of studies investigating the effect of various statins on CEC have been inconsistent (19-21). Furthermore, statins have been shown to induce significant perturbations in gene expression of human peripheral blood mononuclear cells (PBMC) (22,23) and reduce the macrophage content of mouse plaques by promoting macrophage migration from the lesions through stimulation of the C-C chemokine receptor type 7 (CCR7) emigration pathway (24).

Although our recently reported YELLOW (Reduction in Coronary Yellow Plaque, Lipids and Vascular Inflammation by Aggressive Lipid Lowering) trial demonstrated a reduction in lipid content of an obstructive non-culprit lesion (NCL) by NIRS after short-term high-dose statin therapy (9), the YELLOW II study was designed to assess changes in plaque morphology of an obstructive NCL by OCT and NIRS/IVUS with a comprehensive evaluation of HDL functionality, PBMC transcriptomics, and macrophage migration in patients receiving high-dose statin therapy.

METHODS

The protocol of this prospective single-center study was approved by the institutional review board. All patients provided written informed consent. An independent data and safety monitoring board oversaw the conduct, safety, and efficacy of the study. The primary objectives were to examine changes in lipid content of the obstructive NCL, measured by NIRS, and plaque morphology, assessed by OCT; and to compare changes in lipid content and plaque morphology with changes in LDL, HDL, apo A-I, and macrophage functionality. Secondary endpoints included finding correlations between the changes in plaque morphology, CEC, and perturbations in PBMC transcriptome. **Figure 1** shows the study design (study protocol is shown in the [Online Appendix](#)). Stable patients scheduled for elective coronary angiography and/or coronary artery stenting

ABBREVIATIONS AND ACRONYMS

ABCA1 = ATP-binding cassette A1 transporter

CEC = cholesterol efflux capacity

FCT = minimal fibrous cap thickness

hsCRP = high-sensitivity C-reactive protein

IVUS = intravascular ultrasonography

NCL = nonculprit lesion

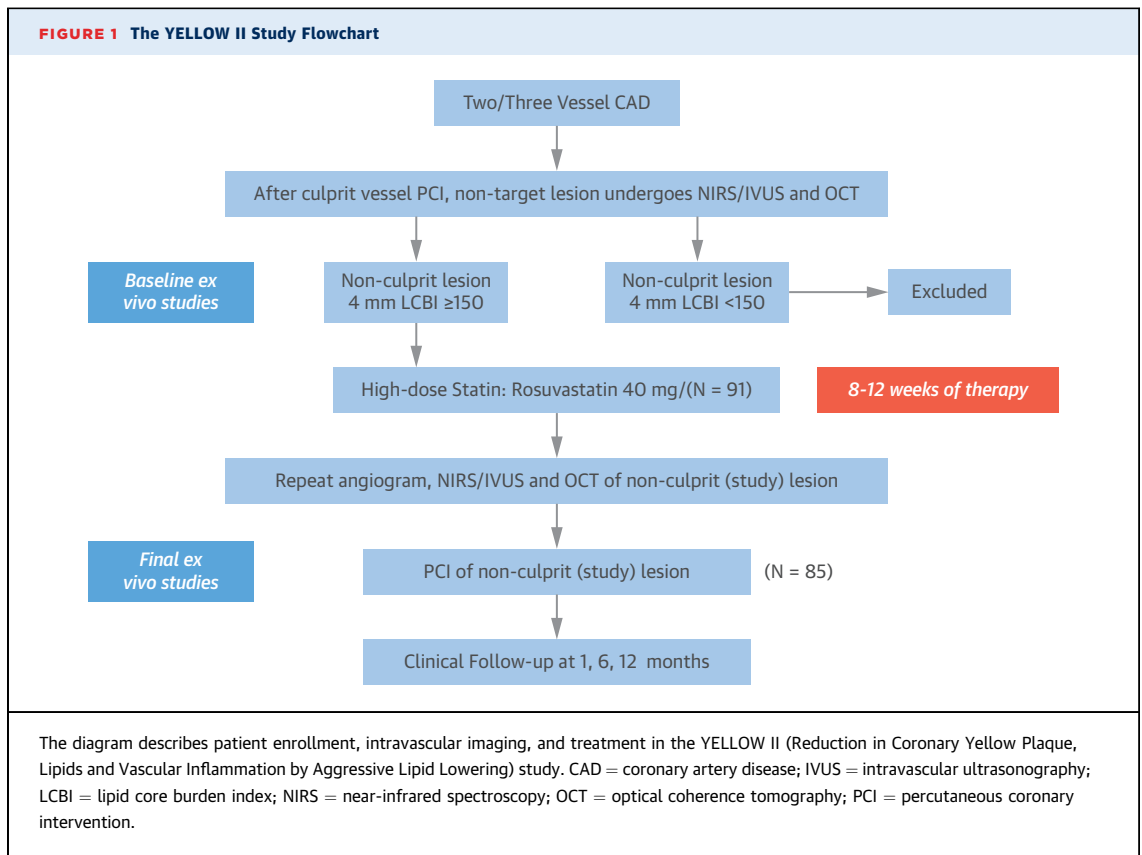
NIRS = near infrared spectroscopy

OCT = optical coherence tomography

PBMC = peripheral blood mononuclear cells

AstraZeneca. Drs. Shameer, Johnson, Kidd, Readhead, and Dudley are supported by grants from National Institutes of Health/ National Institute of Diabetes and Digestive and Kidney Diseases (R01DK098242); National Cancer Institute (U54CA189201); Illuminating the Druggable Genome; Knowledge Management Center sponsored by NIH Common Fund; NCI (U54-CA189201-02); and a National Center for Advancing Translational Sciences and Clinical and Translational Science Award (UL1TR000067). Dr. Dudley is a consultant for or has received honoraria from Janssen Pharmaceuticals, GlaxoSmithKline, AstraZeneca, and Hoffman-La Roche; is a scientific advisor to LAM Therapeutics; and holds equity in NuMedii Inc., Ayasdi Inc., and Ontomics, Inc. All other authors have reported that they have no relationships relevant to the contents of this paper to disclose. Adnan Chhatriwalla, MD, served as Guest Editor for this paper.

Manuscript received October 18, 2016; revised manuscript received October 24, 2016, accepted October 24, 2016.



were screened for this study. The final target population consisted of patients with multivessel disease requiring staged intervention (culprit vessel initially, nonculprit vessel later) with maximal lipid core burden index in a 4-mm length of artery (maxLCBI4mm) >150 by NIRS imaging of the NCLs.

From August 2013 to February 2015, we enrolled 91 patients who had multivessel coronary artery disease, who underwent percutaneous coronary intervention for a culprit lesion, followed by OCT and NIRS/IVUS imaging of an obstructive NCL. Following enrollment, all subjects received rosuvastatin, 40 mg daily. Eight to 12 weeks after enrollment, the NCL was reimaged as a part of staged intervention. All procedures were performed at Mount Sinai catheterization laboratory (New York, New York). Serial changes of serum lipids, high-sensitivity C-reactive protein (hsCRP), and apolipoproteins were assessed at baseline and at follow-up procedures. Additionally, fasting blood samples were obtained during baseline and at follow-up for CEC quantification and PBMC isolation. Off-line gray-scale IVUS, NIRS, and OCT analyses were performed at the Cardiovascular Research Foundation (New York, New York), which had no knowledge of the patients' clinical presentation. The observed changes in plaque morphology by intravascular imaging were related to the

changes in CEC and messenger ribonucleic acid (mRNA) expression of PBMC. Statistical analyses were performed by the data coordinating center at Cardiovascular Institute of Mount Sinai Hospital, also blinded to clinical data.

IMAGE ACQUISITION. OCT image acquisition was performed using the C7-XR OCT model (Intravascular Imaging System; St. Jude Medical, Minneapolis, Minnesota), with continuous intracoronary contrast injection. A TVC (True Vessel Characterization) imaging system with the TVC Insight catheter (Infraredx, Burlington, Massachusetts) was used to perform combined IVUS and NIRS image acquisition for the same lesion ([Online Appendix](#)).

Offline gray-scale IVUS and NIRS analyses were performed according to criteria of the American College of Cardiology consensus statement on IVUS (25) as previously described (9) ([Online Appendix](#)).

OCT images were analyzed systematically at 1-mm intervals according to previously validated criteria for plaque characterization, using the St. Jude Medical offline review workstation ([Online Appendix](#)) (26). Thin-cap fibroatheroma (TCFA) was defined as lipid-rich plaque with minimal FCT <65 μ m.

TRANSLATIONAL STUDIES. Cholesterol efflux capacity was quantified by measuring the efflux of

radiolabeled cholesterol from mouse cell line J774 macrophages to patient apo B-depleted serum as previously described (Online Appendix) (17,19). To correct for interassay variation across plates, control serum pooled from 18 healthy volunteers was included on each plate; CEC values for patient sera samples were normalized to the pooled value. The interassay coefficient of variation was 2.7%. Additional details regarding migration assay, gene expression profiling, and differential expression profiling are given in the Online Appendix.

STATISTICAL ANALYSIS. Sample size was calculated as described in the study protocol in the Online Appendix. All continuous measurements were expressed as mean ± SD for normally distributed variables or median and interquartile ranges for nonparametric data. The Shapiro-Wilk test was used to assess the normality of continuous data. Differences between baseline and follow-up measurements were assessed using the Wilcoxon signed rank test. The changes in biochemical parameters and CEC after therapy were calculated by subtracting the baseline values from those at follow-up. Linear regression was used to estimate the correlates of the change in minimal FCT. Sensitivity analysis was performed to assess the effect of statin exposure at baseline, using statistical interaction testing by including an interaction term in the models. All reported p values are 2-tailed with a value of <0.05 indicating statistical significance. Analyses were performed using SAS version 9.4 software (SAS Institute, Cary, North Carolina). Probability values of gene ontology terms, functional classes, and pathway enrichment using differential expression profile and weighted gene co-expression network analysis (WGCNA) modules were reported after multiple testing correction.

RESULTS

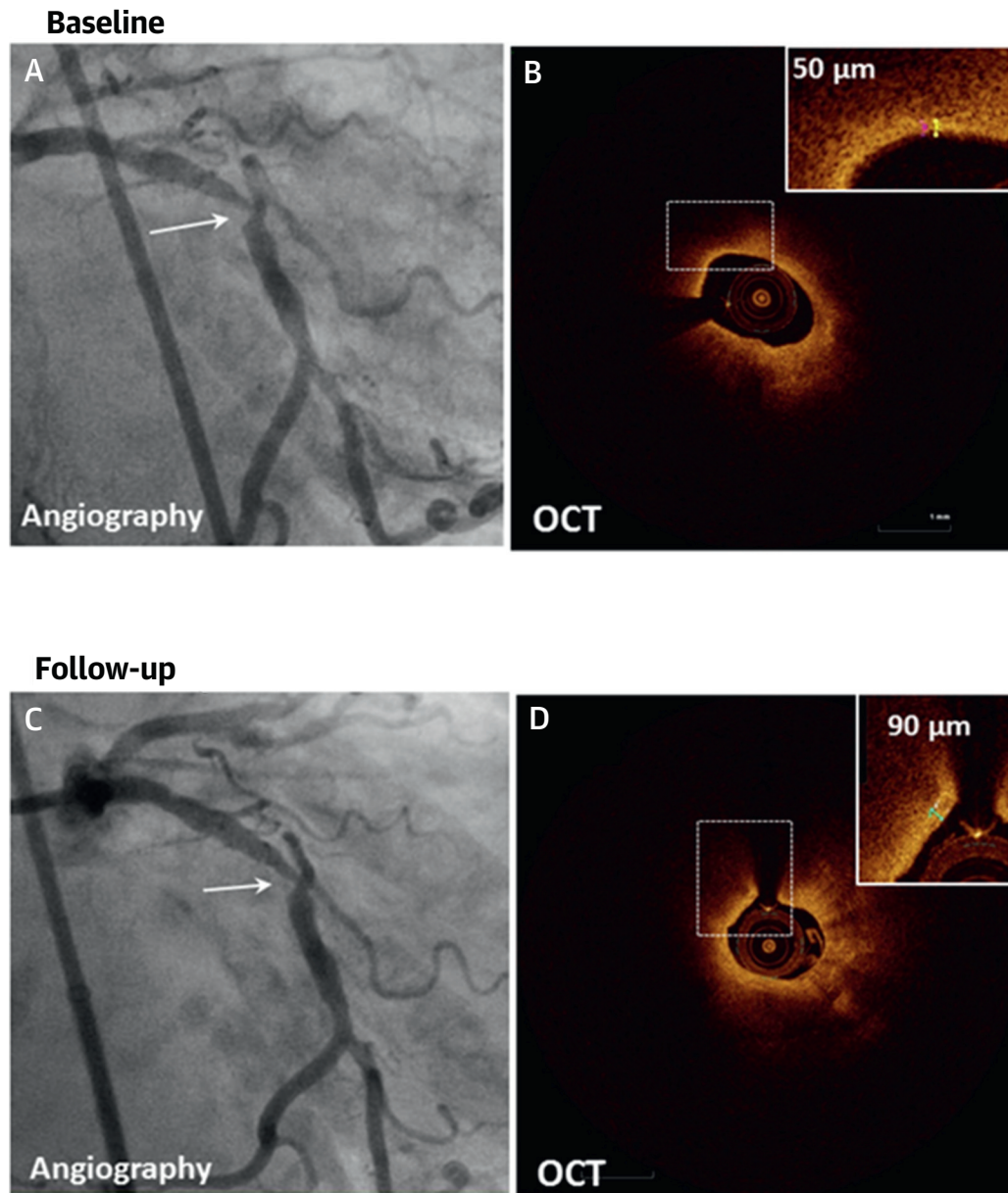
From August 2013 until February 2015, 962 consecutive patients with chronic stable angina presenting for elective coronary angiography were screened and gave consent. After we applied clinical (n = 31), angiographic (n = 834), and NIRS (n = 6) exclusion criteria, 91 patients were enrolled in the study (Online Figure 1). Six patients were lost to follow-up. A total of 85 plaques from 85 patients were evaluated using NIRS/IVUS and OCT at baseline and follow-up. In these 85 patients, 3 OCT pullback images (1 baseline, 2 follow-up) needed to be excluded from the analysis due to poor image quality. Baseline demographic characteristics, concomitant medications, and treated vessel information for the study patients are shown in Online Table 1. Sixty-nine (81%) of the 85 patients

TABLE 1 Chemical Parameters, CEC, and Intravascular Imaging

	Baseline (n = 85)	Follow-Up (n = 85)	p Value
Total cholesterol, mg/dl	153.3 ± 44.9	115.0 ± 29.9	<0.001
LDL cholesterol, mg/dl	86.8 ± 39.6	50.6 ± 25.0	<0.001
HDL cholesterol, mg/dl	41.2 ± 12.7	42.2 ± 13.1	0.41
Triglyceride, mg/dl	128.6 ± 111.8	107.8 ± 66.7	0.04
apo B, mg/dl	79.6 ± 28.0	57.4 ± 17.5	<0.001
apo A-I, mg/dl	120.1 ± 25.6	126.9 ± 23.3	0.004
hsCRP, mg/l	3.5 ± 5.5	2.7 ± 4.2	<0.001
CEC	0.81 ± 0.14	0.84 ± 0.14	0.003
OCT			
Reference lumen CSA, mm ²	6.8 ± 2.2	6.6 ± 2.1	0.07
Minimum lumen CSA, mm ²	1.80 ± 0.69	1.84 ± 0.68	0.26
Area stenosis, %	71.9 ± 8.5	70.1 ± 9.0	0.24
Lipid rich plaque	75 (88.2)	72 (84.7)	0.50
Lipid arc maximum, °	147.2 ± 80.1	139.2 ± 79.4	0.20
Lipid length, mm	5.8 ± 5.2	4.9 ± 4.0	0.03
Lipid volume index, ° × mm*	663.7 ± 668.6	586.8 ± 616.5	0.16
Minimum cap thickness, μm	100.9 ± 41.7	108.6 ± 39.6	<0.001
TCFA†	17 (20.0)	6 (7.1)	0.003
Macrophages	83 (97.6)	80 (94.1)	0.50
Macrophage arc maximum, °	136.2 ± 66.6	129.1 ± 60.5	0.11
Macrophage length, mm	9.8 ± 5.4	8.8 ± 5.1	<0.001
Thrombus	15 (17.6)	12 (14.1)	0.51
Microvessel	64 (75.3)	66 (77.6)	0.63
Calcium deposition	75 (88.2)	74 (87.1)	0.71
Calcium arc maximum, °	124.4 ± 85.6	127.6 ± 86.2	0.05
IVUS			
EEM volume, mm ³	298.2 ± 147.3	297.4 ± 148.8	0.73
TAV, mm ³	182.3 ± 94.5	182.7 ± 95.5	0.82
PAV, %	60.71 ± 7.52	60.97 ± 7.57	0.30
Plaque burden, %	75.93 ± 7.07	75.79 ± 7.96	0.78
Plaque plus media, mm ²	7.67 ± 3.32	7.75 ± 3.44	0.52
NIRS			
maxLCBI _{4mm}	416.6 ± 172.9	400.2 ± 180.4	0.43

Values are mean ± SD or n (%). *Averaged lipid arc × lipid length. †Lipid-rich plaque with the minimal fibrous cap thickness <65 μm.
 apo = apolipoprotein; CEC = cholesterol efflux capacity; CSA = cross-sectional area; EEM = external elastic membrane; HDL = high-density lipoprotein; hsCRP = high-sensitivity C-reactive protein; IVUS = intravascular ultrasonography; LDL = low-density lipoprotein; maxLCBI_{4mm} = maximal lipid core burden index in a 4-mm segment; NIRS = near-infrared spectroscopy; OCT = optical coherence tomography; PAV = percentage of atheroma volume; TAV = total atheroma volume; TCFA = thin-cap fibroatheroma.

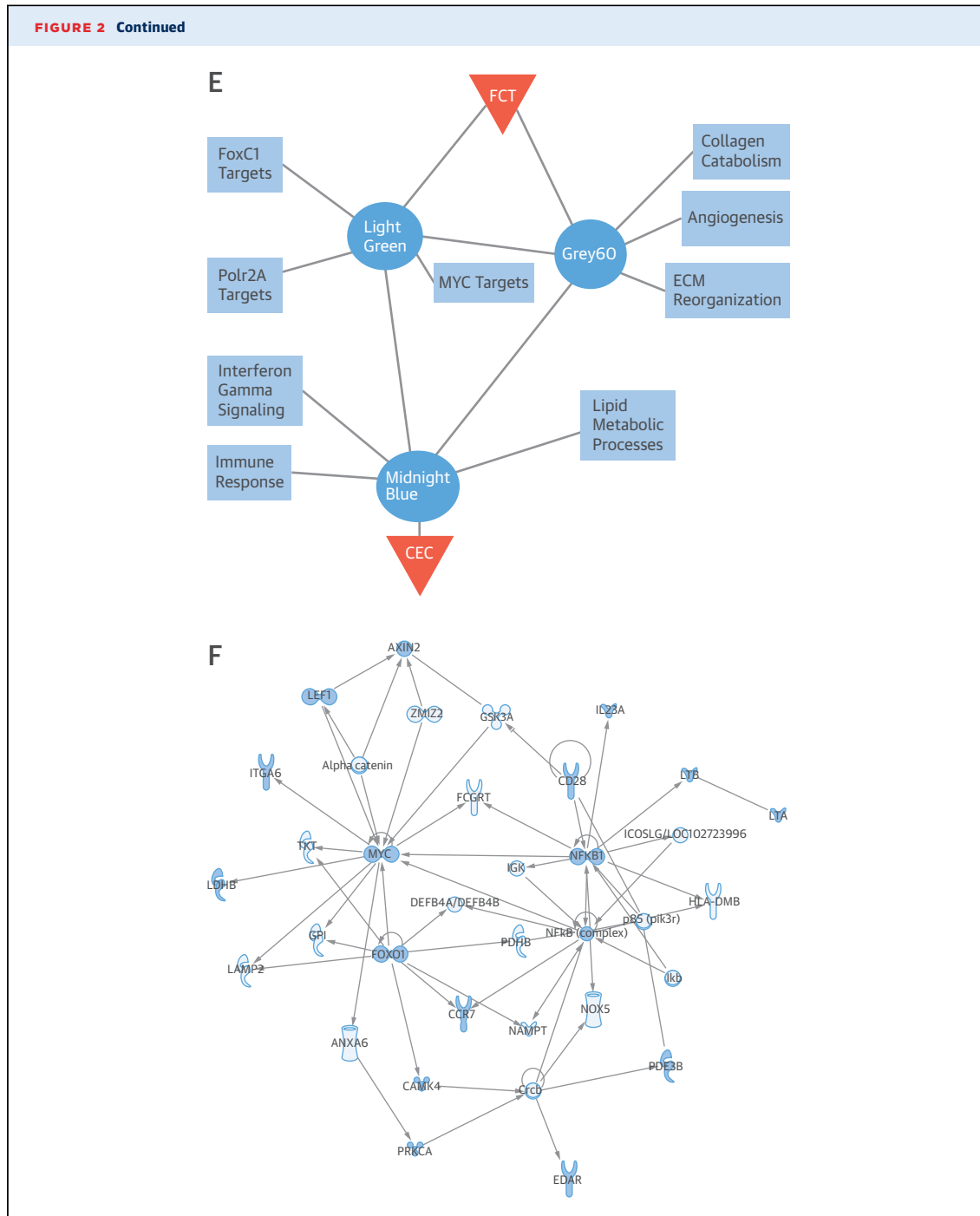
were already receiving statin therapy; 16 patients (19%) were statin-naïve. After patients received intensive statin therapy, there were significant reductions from baseline in total cholesterol, LDL-C, and triglyceride levels but no significant change in HDL-C (Table 1). Additionally, while apo A-I levels significantly increased, apo B and hsCRP levels decreased significantly after treatment. During 1-year follow-up, there was no cardiac-related death in the study population (Online Table 2). Most frequent events were hospitalization for chest pain (17.6%) and urgent revascularization (15.3%); 3 patients had nonfatal myocardial infarctions.

FIGURE 2 Intravascular Imaging and Mediators of CEC and FCT

Continued on the next page

IMAGING RESULTS. Baseline and follow-up multimodal imaging findings are summarized in Table 1 and Online Tables 3 to 6. Baseline OCT-verified minimal FCT was $100.9 \pm 41.7 \mu\text{m}$, which was increased at

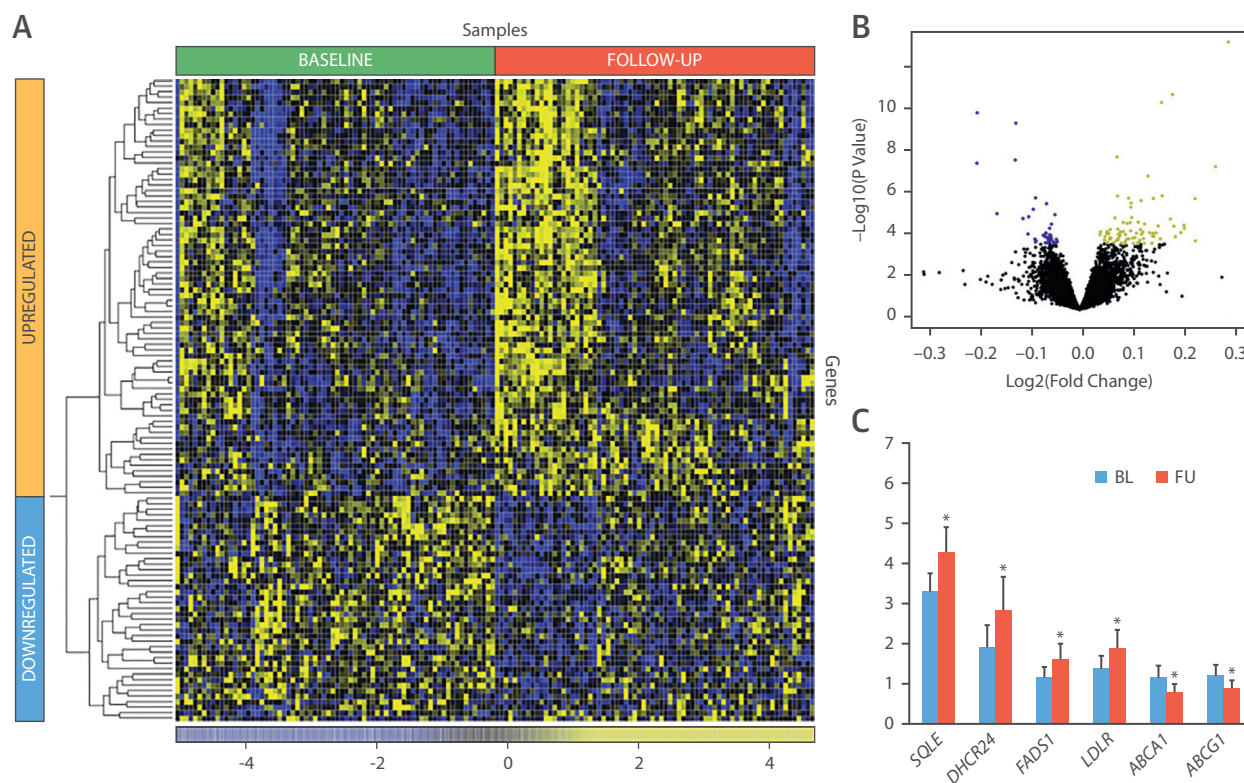
follow-up to $108.6 \pm 39.6 \mu\text{m}$ ($p < 0.001$), with the average change of $9.1 \pm 17.1 \mu\text{m}$. TCFA prevalence decreased from 20.0% to 7.1% ($p = 0.003$) (Figures 2A to 2D). Online Table 7 describes



demographics and risk factors for 3 groups of patients, who demonstrated an increase (n = 39), a decrease (n = 13), or no change (n = 18) in FCT at follow-up. Additionally, there was a significant decrease in lipid length with a trend toward a reduction in maximal lipid arc; similarly, OCT-derived macrophage length significantly reduced after statin therapy with a trend toward a decrease in

maximal macrophage arc (Table 1). Upon follow-up, IVUS-based total atheroma volume, percentage of atheroma volume, and NIRS maxLCBI4mm did not reveal significant changes (Table 1).

TRANSLATIONAL RESULTS. After high-dose statin therapy, CEC of apo B-depleted sera from study participants normalized to a pool of healthy controls

FIGURE 3 Transcriptomic Landscape of Differentially Expressed Genes in PBMCs

(A) In this differential expression heat map of 117 differentially expressed genes, baseline data are demarcated. **(B)** Volcano plot with 9,978 genes tested in the differential expression, where **yellow** = upregulated genes; **blue** = downregulated genes. **(C)** We performed quantitative reverse transcription-polymerase chain reaction (RT-PCR) analysis of peripheral blood mononuclear cells gene expression at baseline and follow-up for a subgroup of 24 study patients. Consistent with microarray data, the messenger ribonucleic acid abundance levels of *SQLE*, *DHCR24*, *FADS1*, and *LDLR* increased significantly and those of *ABCA1* and *ABCG1* decreased significantly after statin therapy compared to levels at baseline. Data are mean \pm SE of mean of duplicates of RT-PCR reactions. * $p < 0.05$. BL = baseline; FU = follow-up.

increased significantly (**Table 1**) with an average change of 0.04 ± 0.08 . Cholesterol efflux capacity increased in 50 and decreased in 32 patients compared to the baseline, whereas 3 patients did not demonstrate a change in CEC (**Online Table 8** describes demographics and risk factors according to changes in CEC at follow-up). The change in FCT was greater in patients who had increased CEC at follow-up compared to those who demonstrated a decrease or no change in CEC at follow-up ($13.3 \pm 15.3 \mu\text{m}$ vs. $5.1 \pm 18.6 \mu\text{m}$, respectively; $p = 0.043$).

We also assessed whether beneficial changes in plaque morphology by intravascular imaging after statin therapy were associated with the changes in macrophage functionality (27,28). Macrophage chemotaxis toward CCL19 and CCL21 was measured using mouse cell line J774 pretreated with apo B-depleted serum of study participants. There were no differences between the number of migrated cells at

baseline and the number after 8 to 12 weeks of high-dose statin therapy with the mean change in the normalized number of migrated cells 0.19 ± 1.2 , as shown in **Online Figure 2**.

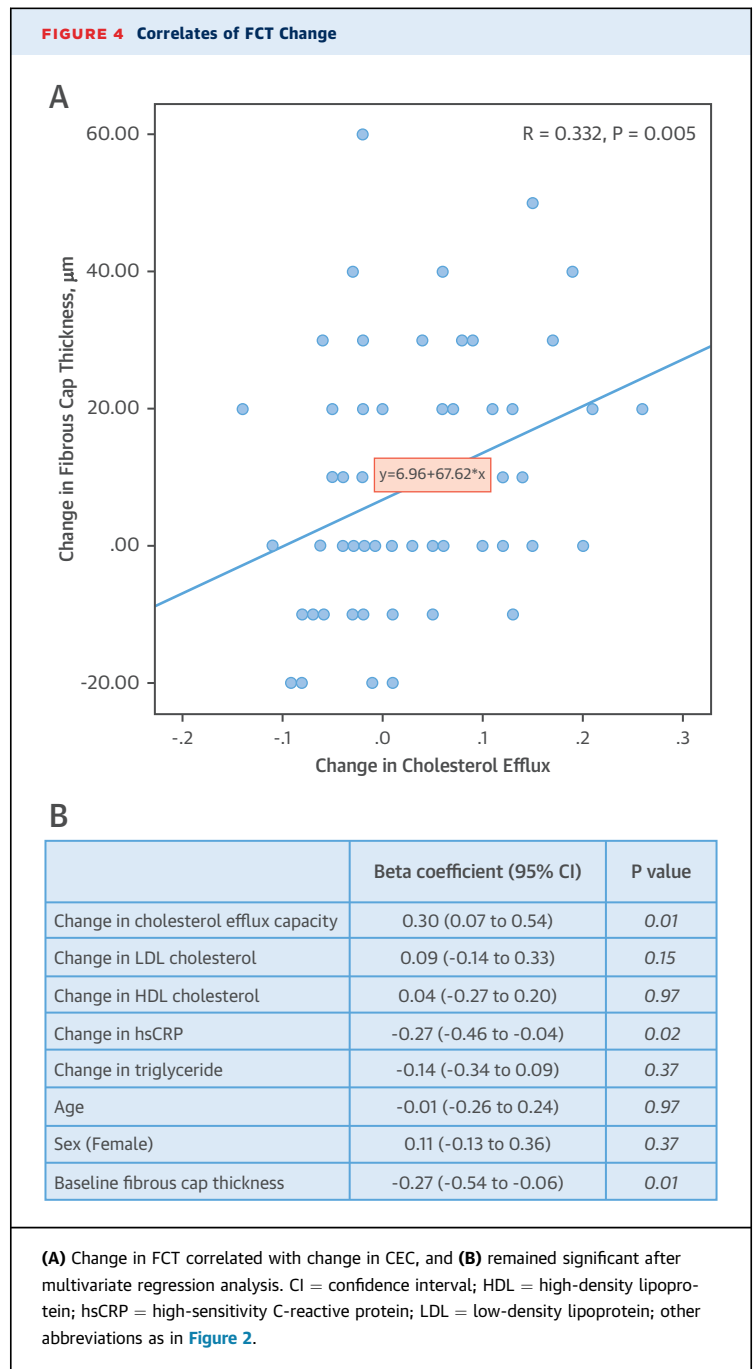
In addition to translational cell biology experiments, transcriptomic profile of PBMC was analyzed at baseline and at follow-up to identify differentially expressed signature (**Figures 3A and 3B**, **Online Appendix**). A total of 29,377 probes mapping to 20,819 genes were assayed using microarray technology. After we normalized data, assessed quality control, and removed nonexpressed genes, 981 probes mapping to a total of 9,978 genes were retained to identify the differential expression profile. The differential expression profile identified 117 genes (78 upregulated and 39 downregulated), which play critical biological functions related to cholesterol metabolism, inflammation pathways, matrix degradation, and cholesterol regulation and statin metabolism.

Following biocuration and pathway enrichment analyses, a panel of 6 genes with the lowest p values was used for reverse-transcription polymerase chain reaction (RT-PCR) assay. These genes play key biological roles related to cholesterol synthesis (*SQLE*), regulation of fatty acids unsaturation (*FADS1*), cellular cholesterol uptake (*LDLR*), efflux (*ABCA1*, *ABCG1*), and lowering of inflammatory processes (*DHCR24*) and are thus involved in cross-talk between statin metabolism and cholesterol synthesis pathways (29). The observed perturbations were confirmed by RT-PCR (Figure 3C). The gene expression profile and confirmatory assays provide a molecular portrait of factors driving phenotypic changes including efflux and increase in FCT.

By using univariate regression analysis, we correlated the changes in minimal FCT with the changes in CEC ($R = 0.332$; $p = 0.005$) (Figure 4A) and hsCRP ($R = -0.324$; $p = 0.007$) but not with changes in serum LDL-C ($R = 0.033$; $p = 0.79$), HDL-C ($R = 0.096$; $p = 0.43$), and triglyceride ($R = -0.034$; $p = 0.78$) levels. The associations of FCT with CEC and with hsCRP remained significant after adjusting for age, sex, and changes in lipid levels (Figure 4B). Minimal cap thickness at baseline was another independent predictor of FCT change after high-dose statin therapy. Baseline statin therapy was not an independent covariate of the change in FCT (Online Figure 3B). The correlation between change in FCT and CEC was higher in statin-naïve patients than in patients exposed to statins at baseline ($R = 0.739$; $p = 0.001$ vs. 0.200, respectively; $p = 0.15$) (Online Figure 3A). Statin therapy at baseline had a significant dampening effect ($\beta = -0.53$; 95% confidence interval [CI]: -1.1 to -0.09 ; $p = 0.02$) on the association between the changes in FCT and CEC (Online Figure 3B).

The change in macrophage migration did not correlate with the change in FCT ($R = -0.11$; $p = 0.38$); however, there was a significant interaction between migration and baseline exposure to statin ($\beta = -0.68$; 95% CI: -1.2 to -0.11 ; $p = 0.02$) (Online Figure 3D) with a slightly stronger correlation detected in statin-naïve patients (Online Figure 3C).

Comparative analyses of the phenotypes and gene-expression data using WGCNA revealed 12 significant modules (Figures 2E and 2F, Online Figure 4, Online Appendix). The increase in CEC was associated with the midnight blue module of 65 genes (Figure 2F). Genes in this module were enriched for inflammatory response pathways (*IL23A*, *CD28*, *LTA*, *CCR7*, and *PRKCA*), cellular adhesion (*DPP4*, *PDE3B*, *LEF1*, *ITGA6*, *CCR7*, *PRKCA*, and *EPHA1*), regulation of lipid metabolic processes (*CRTC3*, *EPHX2*, *PDE3B*, *CCR7*, and *NFKB1*), Fc epsilon receptor (*FCERI*) signaling (*TRAT1*, *CD28*, *FOXO1*, and *NFKB1*), and cytokine



receptor interactions (*EDAR*, *IL11RA*, *IL23A*, *LTA*, *CD27*, *FLT3LG*, *CCR*, and *LTB*). Genes in the correlated module of CEC including chemokine receptors are hallmarks of immune-inflammatory response to the presence of cholesterol and its efflux (30-32). Biological significance and functional roles of differentially expressed genes and the modules associated with CEC and FCT are provided in the Online Appendix (including Online Figures 5 to 13 and biological interpretation of differentially expressed genes).

Changes in FCT were associated with 2 modules, gray60 (n = 40 genes) and light green (n = 37 genes). Collectively these gene sets were associated with interferon signaling and inflammatory processes (*ORM1*, *HP*, *CHI3L1*, *OLR1*, *AZU1*, and *ELANE*). Genes in gray60 modules were localized to the cellular regions of matrix assembly (*COL17A1*, *CTSG*, *MMP8*, *MMP9*, and *ELANE*), extracellular matrix organization (GO:0030198, *COL17A1*, *CTSG*, *MMP8*, *MMP9*, and *ELANE*), and extracellular matrix (GO:0031012, *SLPI*, *CRISP3*, *TFF3*, *CHI3L1*, *PRTN3*, *CTSG*, *DEFA1*, *MMP8*, and *MMP9*), suggesting a role for matrix remodeling and change in FCT. Although the roles of matrix metalloproteinases and collagens in plaque stability are known, the prospective roles of additional classes of genes including *CTS* and *ELANE* are evolving and need further study (33-35).

DISCUSSION

The time interval for aggressive statin treatment in the present study was only 8 to 12 weeks, and morphological changes in atherosclerotic plaques were evaluated and compared with CEC, macrophage functionality, and gene expression changes in PBMC. Although we did not observe a significant change in plaque lipid content quantified using NIRS, we did detect a significant increase in FCT of obstructive NCLs and enhancement of CEC in patients with stable coronary artery disease (Central Illustration). Moreover, our results demonstrated a strong and independent association between fibrous cap thickening and improved CEC. In concert, these findings suggested that macrophage cholesterol efflux may contribute to short-term plaque stabilization soon after initiation of intensive statin therapy, a process that appears to be independent of any changes in plaque lipid content or serum cholesterol. Remarkably, after a short duration of statin therapy, the prevalence of TCFA was reduced from 20.0% to 7.1% ($p = 0.003$).

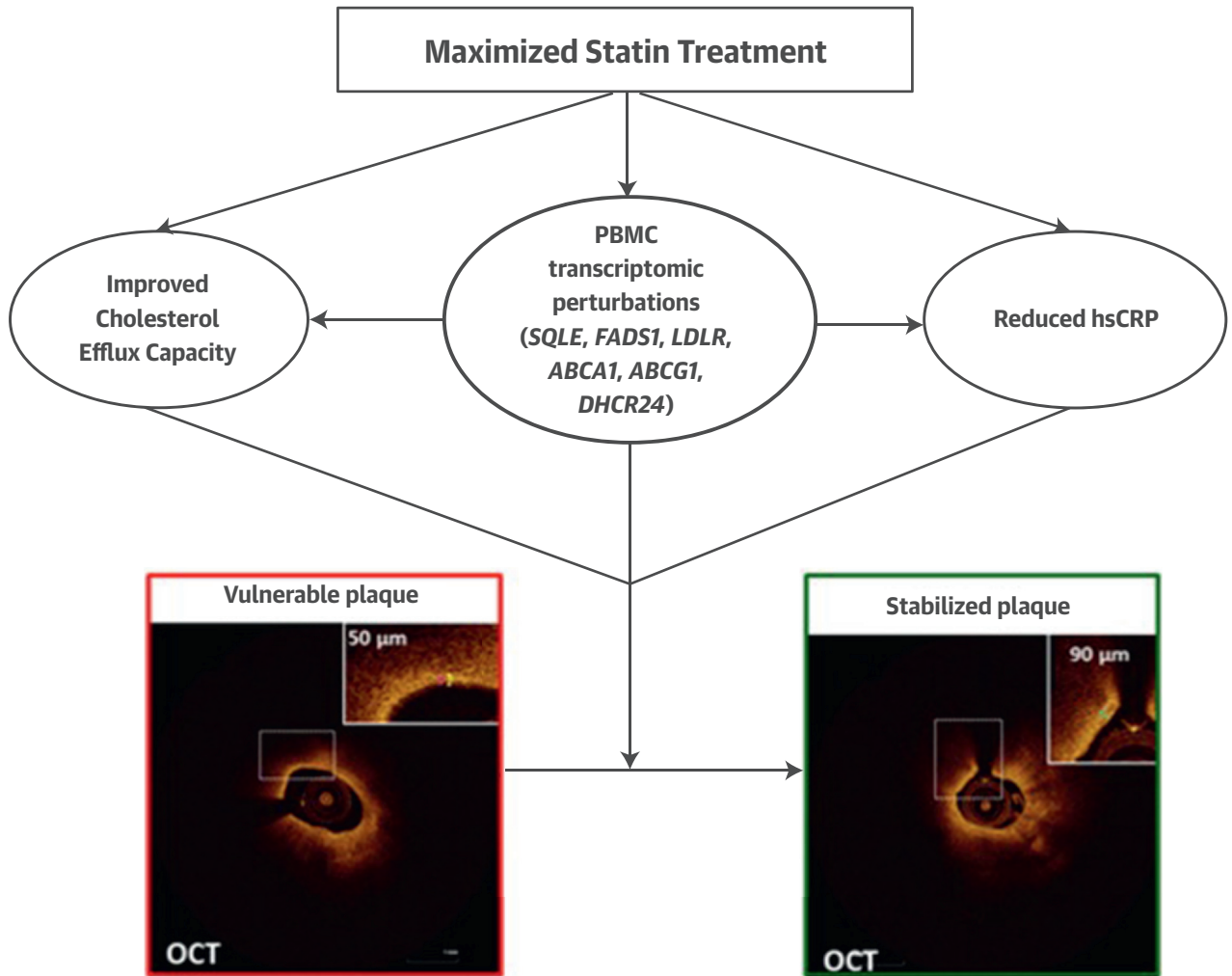
The central role of ABCA1-mediated macrophage cholesterol efflux to antiatherogenic properties of HDL-C has been demonstrated by multiple clinical and preclinical studies. Patients with ABCA1 loss-of-function mutations have lower CEC and greater intima-media thickness than controls (36). Our results demonstrated a relationship between CEC and plaque stabilization (Figure 4) and an association between HDL-C function and plaque stabilization in patients that has not been shown previously. The experimental evidence, however, is strong, and mice deficient in ABCA1/ABCG1 efflux transporters have not only accelerated atherosclerosis but also

increased secretion of inflammatory cytokines, apoptosis, and increased expression of inflammatory genes (37).

Statin effects on CEC is extremely controversial. Rosuvastatin has been associated with reductions in total CEC and ABCA1-mediated efflux in 2 studies (21,38). Atorvastatin had no significant effect on CEC in 1 study (21), whereas a smaller study showed a significant reduction in ABCA1-mediated CEC (20). Simvastatin produced a significant increase in non-ABCA1-mediated CEC and a trend toward increase in ABCA1-mediated CEC (39), whereas a more recent, larger study suggested the opposite effect (21). The effects of pitavastatin are limited to a single study showing an increase in PEGHDL-specific efflux by using a unique modified CEC assay (40). Therefore, statin therapy in previous studies had either minimal impact or was associated with decreased CEC. Due to the absence of a control arm, we found it impossible to assess the effect of rosuvastatin on CEC.

In the present study, we also explored the relationship between changes in PBMC transcriptome and changes in plaque morphology and CEC in patients undergoing intensive statin treatment (Figure 3). Of 117 differentially expressed genes, 6 genes (*SQLE*, *DHCR24*, *FADS1*, *LDLR*, *ABCA1*, and *ABCG1*) were most strongly associated with favorable outcomes in terms of FCT and CEC and were validated using RT-PCR. These differentially expressed genes play critical biological functions related to cholesterol metabolism, signal transduction pathways, inflammation, and statin metabolism (Figure 3). Among the differentially expressed genes, *SQLE* catalyzes the first oxygenation step in sterol biosynthesis; this step is categorized as one of the crucial rate-limiting enzymes in this pathway (41). It could be hypothesized that *SQLE* upregulation indicates maximum effective statin dose through maximum suppression of HMG-CoA (3-hydroxy-3-methyl-glutaryl-coenzyme A reductase). It is possible that maximization of statin in a given patient determines the efficacy of treatment for plaque stabilization. The *DHCR24* gene encoding a terminal enzyme in cholesterol synthesis (42) also mediates the inhibition of vascular inflammation by lipid-free apo A-I (43). Significant upregulation of *DHCR24* expression and reduction of hsCRP levels in our study supported a potential anti-inflammatory role for *DHCR24*. While upregulation of *LDLR* is expected and understandable, the downregulation of *ABCA1* and *ABCG1* expression is intriguing in the setting of significantly enhanced CEC. It is, however, consonant with all previous reports that have demonstrated association of statin treatment with an increase in cholesterol uptake and suppression of apo A-related

CENTRAL ILLUSTRATION High-Intensity Statins and Intracoronary Imaging, Cholesterol Efflux, and Transcriptome Perturbations



Kini, A.S. et al. *J Am Coll Cardiol.* 2017;69(6):628-40.

In patients with stable coronary artery disease, we detected a significant increase in fibrous cap thickness of obstructive coronary lesions by OCT, enhancement of CEC, reduction in hsCRP level, and significant perturbations in the PBMC transcriptome after 8 to 12 weeks of rosuvastatin 40 mg daily. Improved macrophage CEC and reduced hsCRP contributed to plaque stabilization independently of changes in serum cholesterol. Furthermore, the significant transcriptomic perturbations related to cholesterol synthesis, regulation of fatty acid unsaturation, cellular cholesterol uptake, efflux, and inflammation may cooperate in determining statin's beneficial effects on plaque stabilization. CEC = cholesterol efflux capacity; hsCRP = high-sensitivity C-reactive protein; OCT = optical coherence tomography; PBMC = peripheral blood mononuclear cell.

ABCA1 cassette protein expression of CEC through sterol regulatory element-binding protein 2 (SREBP2); the transcription factor SREBP2 is activated by low cellular cholesterol (44). Similar to *SQLE*, the expression levels of *ABCA1* and *ABCG1* may provide a quantitative measurement for efficacy of patient-specific effects of statin on plaque morphology. Although

several genocopies of *LDLR* are associated with inter-individual variation in cardiac risk and cholesterol metabolism, the precise roles of *SQLE* and *DHCR24* remain unknown, and specifically designed resequencing or association studies with these genes would reveal their pharmacogenomic contributions in the statin response pathways. As shown by several

studies, we believe the PBMC gene expression will be very similar to that of atherosclerotic plaque (45,46). A mature technology, global gene expression profiling provides a snapshot of gene expression from a given set of sample/tissues in the setting of a disease, drug perturbations, or other biological conditions. Meta-analyses of 238 diseases and 122 tissues from 8,435 microarrays have shown the robustness of gene expression signatures across tissues and experiments in numerous settings, including several cardiovascular diseases (47). We expect minor degrees of difference might be present but cannot be ascertained without blood-versus-tissue comparison. However, the core set of genes and the direction remain robust, and the gene expression signature is now regarded as a major analytical method in personalized medicine (48,49).

High macrophage content is an important feature of vulnerable plaques; reducing macrophage accumulation contributes to the positive influence of lipid lowering. The mechanisms involved in macrophage clearance are a subject of active debate. Statins contributed to a significant reduction in mouse plaque macrophages through stimulation of the CCR7 emigration pathway (24). The present study revealed significant reduction of OCT-detected macrophage accumulation in lesions but did not demonstrate a change in the migration of J774 mouse macrophages pretreated with patient serum toward CCR7 ligands CCL19 and CCL21. A possible explanation for the negative finding was that our *in vitro* model was not able to reflect all the complexities of plaque macrophage in the *in vivo* environment. Conversely, the results might suggest that different mechanisms are responsible for the reduction of plaque macrophage content, including reduction in monocyte recruitment and local apoptosis (50), improved endothelial barrier function for LDL entry (51), and reversed phenotypic changes of macrophage-appearing cholesterol-loaded vascular smooth muscle cells (52).

STUDY LIMITATIONS. The lack of a randomized design precluded causal inferences between the use of high-intensity statins and the changes observed in various morphologic, functional, and genetic parameters. Duration of follow-up was also short and not likely to demonstrate the striking changes in plaque morphology. A prospectively designed randomized study in the next phase should compare the continuation of statin therapy with dose maximization on these important morphological and mechanistic endpoints. Unlike our previous YELLOW (Reduction in Coronary Yellow Plaque, Lipids and

Vascular Inflammation by Aggressive Lipid Lowering) study, the present experiment did not demonstrate significant reductions in NIRS-based lipid core burden index, a null result possibly attributable to a NIRS-based inclusion criterion in the YELLOW II protocol and the lack of a comparative standard dose arm. Although we have separately listed all individual correlations of morphological changes with biochemical, cell biological, and genomic perturbations in our study protocol, we have highlighted the positive correlation more extensively in the discussion section especially pertaining to CEC and transcriptomic results. The role of several time-varying covariates that could be potential confounders, including changes in smoking, alcohol intake, physical activity, and diet, were not considered in the study.

CONCLUSIONS

We observed favorable modulation in different markers of coronary atherosclerotic plaque vulnerability among patients treated with high-intensity statins for a short duration. In part, these changes may be attributable to enhanced CEC, an independent correlate of increased FCT in our study. We also demonstrated that significant transcriptomic perturbations related to cholesterol synthesis, regulation of fatty acid unsaturation, cellular cholesterol uptake, efflux, and inflammation may cooperate in determining statin's beneficial effects on plaque stabilization.

ADDRESS FOR CORRESPONDENCE: Dr. Annapoorna S. Kini, Department of Interventional Cardiology, Mount Sinai Hospital, One Gustave L. Levy Place, Box 1030, New York, New York 10029. E-mail: annapoorna.kini@mountsinai.org.

PERSPECTIVES

COMPETENCY IN MEDICAL KNOWLEDGE: FCT of obstructive NCLs assessed by OCT and CEC increased in patients with stable coronary disease treated with high-dose rosuvastatin.

TRANSLATIONAL OUTLOOK: Additional research is needed to understand how macrophage cholesterol efflux improves plaque stabilization soon after initiation of intensive statin therapy, which appears independent of changes in plaque lipid content or serum cholesterol levels.

REFERENCES

1. Randomized trial of cholesterol lowering in 4444 patients with coronary heart disease: the Scandinavian Simvastatin Survival Study (4S). *Lancet* 1994;344:1383-9.
2. Prevention of cardiovascular events and death with pravastatin in patients with coronary heart disease and a broad range of initial cholesterol levels. The Long-Term Intervention with Pravastatin in Ischaemic Disease (LIPID) study group. *N Engl J Med* 1998;339:1349-57.
3. Downs JR, Clearfield M, Weis S, et al. Primary prevention of acute coronary events with lovastatin in men and women with average cholesterol levels: results of AFCAPS/TexCAPS. Air Force/Texas Coronary Atherosclerosis Prevention Study. *JAMA* 1998;279:1615-22.
4. Shepherd J, Cobbe SM, Ford I, et al. Prevention of coronary heart disease with pravastatin in men with hypercholesterolemia. West of Scotland Coronary Prevention Study Group. *N Engl J Med* 1995;333:1301-7.
5. Ridker PM, Cannon CP, Morrow D, et al. C-reactive protein levels and outcomes after statin therapy. *N Engl J Med* 2005;352:20-8.
6. Ridker PM, Danielson E, Fonseca FA, et al. Rosuvastatin to prevent vascular events in men and women with elevated C-reactive protein. *N Engl J Med* 2008;359:2195-207.
7. Nicholls SJ, Ballantyne CM, Barter PJ, et al. Effect of two intensive statin regimens on progression of coronary disease. *N Engl J Med* 2011;365:2078-87.
8. Nissen SE, Tuzcu EM, Schoenhagen P, et al. Effect of intensive compared with moderate lipid-lowering therapy on progression of coronary atherosclerosis: a randomized controlled trial. *JAMA* 2004;291:1071-80.
9. Kini AS, Baber U, Kovacic JC, et al. Changes in plaque lipid content after short-term intensive versus standard statin therapy: the YELLOW trial (reduction in yellow plaque by aggressive lipid-lowering therapy). *J Am Coll Cardiol* 2013;62:21-9.
10. Park SJ, Kang SJ, Ahn JM, et al. Effect of statin treatment on modifying plaque composition: a double-blind, randomized study. *J Am Coll Cardiol* 2016;67:1772-83.
11. Hattori K, Ozaki Y, Ismail TF, et al. Impact of statin therapy on plaque characteristics as assessed by serial OCT, grayscale and integrated backscatter-IVUS. *J Am Coll Cardiol Img* 2012;5:169-77.
12. Takarada S, Imanishi T, Kubo T, et al. Effect of statin therapy on coronary fibrous-cap thickness in patients with acute coronary syndrome: assessment by optical coherence tomography study. *Atherosclerosis* 2009;202:491-7.
13. Landray MJ, Haynes R, Hopewell JC, et al. Effects of extended-release niacin with laropiprant in high-risk patients. *N Engl J Med* 2014;371:203-12.
14. Barter PJ, Caulfield M, Eriksson M, et al. Effects of torcetrapib in patients at high risk for coronary events. *N Engl J Med* 2007;357:2109-22.
15. Rader DJ, Alexander ET, Weibel GL, Billheimer J, Rothblat GH. The role of reverse cholesterol transport in animals and humans and relationship to atherosclerosis. *J Lipid Res* 2009; Suppl 50:S189-94.
16. Rohatgi A, Khera A, Berry JD, et al. HDL cholesterol efflux capacity and incident cardiovascular events. *N Engl J Med* 2014;371:2383-93.
17. Saleheen D, Scott R, Javad S, et al. Association of HDL cholesterol efflux capacity with incident coronary heart disease events: a prospective case-control study. *Lancet Diabetes Endocrinol* 2015;3:507-13.
18. Mody P, Joshi PH, Khera A, Ayers CR, Rohatgi A. Beyond coronary calcification, family history, and C-Reactive protein: cholesterol efflux capacity and cardiovascular risk prediction. *J Am Coll Cardiol* 2016;67:2480-7.
19. Khera AV, Cuchel M, de la Llera-Moya M, et al. Cholesterol efflux capacity, high-density lipoprotein function, and atherosclerosis. *N Engl J Med* 2011;364:127-35.
20. Ronseim GE, Hutchins PM, Isquith D, Vaisar T, Zhao XQ, Heinecke JW. Niacin therapy increases high-density lipoprotein particles and total cholesterol efflux capacity but not ABCA1-specific cholesterol efflux in statin-treated subjects. *Arterioscler Thromb Vasc Biol* 2016;36:404-11.
21. Nicholls SJ, Ruotolo G, Brewer HB, et al. Cholesterol efflux capacity and pre-beta-1 HDL concentrations are increased in dyslipidemic patients treated with evacetrapib. *J Am Coll Cardiol* 2015;66:2201-10.
22. Tuomisto TT, Lumivuori H, Kansanen E, et al. Simvastatin has an anti-inflammatory effect on macrophages via upregulation of an atheroprotective transcription factor, Kruppel-like factor 2. *Cardiovasc Res* 2008;78:175-84.
23. Rezaie-Majd A, Prager GW, Bucek RA, et al. Simvastatin reduces the expression of adhesion molecules in circulating monocytes from hypercholesterolemic patients. *Arterioscler Thromb Vasc Biol* 2003;23:397-403.
24. Feig JE, Shang Y, Rotllan N, et al. Statins promote the regression of atherosclerosis via activation of the CCR7-dependent emigration pathway in macrophages. *PLoS One* 2011;6:e28534.
25. Mintz GS, Nissen SE, Anderson WD, et al. American College of Cardiology Clinical Expert Consensus Document on standards for acquisition, measurement and reporting of intravascular ultrasound studies (IVUS). A report of the American College of Cardiology Task Force on Clinical Expert Consensus Documents. *J Am Coll Cardiol* 2001;37:1478-92.
26. Tearney GJ, Regar E, Akasaka T, et al. Consensus standards for acquisition, measurement, and reporting of intravascular optical coherence tomography studies: a report from the International Working Group for Intravascular Optical Coherence Tomography Standardization and Validation. *J Am Coll Cardiol* 2012;59:1058-72.
27. Zhou JJ, Wang YM, Lee VW, et al. DEC205-DC targeted DNA vaccines to CX3CR1 and CCL2 are potent and limit macrophage migration. *Int J Clin Exp Med* 2012;5:24-33.
28. Adorni MP, Favari E, Ronda N, et al. Free cholesterol alters macrophage morphology and mobility by an ABCA1 dependent mechanism. *Atherosclerosis* 2011;215:70-6.
29. Martin G, Duez H, Blanquart C, et al. Statin-induced inhibition of the Rho-signaling pathway activates PPARalpha and induces HDL apoA-I. *J Clin Invest* 2001;107:1423-32.
30. Phillips MC. Molecular mechanisms of cellular cholesterol efflux. *J Biol Chem* 2014;289:24020-9.
31. Sorci-Thomas MG, Thomas MJ. High density lipoprotein biogenesis, cholesterol efflux, and immune cell function. *Arterioscler Thromb Vasc Biol* 2012;32:2561-5.
32. Tall AR, Yvan-Charvet L. Cholesterol, inflammation and innate immunity. *Nat Rev Immunol* 2015;15:104-16.
33. Cox ID, Clague JR, Bagger JP, Ward DE, Kaski JC. Endothelial dysfunction, subangiographic atheroma, and unstable symptoms in patients with chest pain and normal coronary arteriograms. *Clin Cardiol* 2000;23:645-52.
34. Lee RT, Libby P. The unstable atheroma. *Arterioscler Thromb Vasc Biol* 1997;17:1859-67.
35. Newby AC, Zaltsman AB. Fibrous cap formation or destruction—the critical importance of vascular smooth muscle cell proliferation, migration and matrix formation. *Cardiovasc Res* 1999;41:345-60.
36. van Dam MJ, de Groot E, Clee SM, et al. Association between increased arterial-wall thickness and impairment in ABCA1-driven cholesterol efflux: an observational study. *Lancet* 2002;359:37-42.
37. Westerterp M, Murphy AJ, Wang M, et al. Deficiency of ATP-binding cassette transporters A1 and G1 in macrophages increases inflammation and accelerates atherosclerosis in mice. *Circ Res* 2013;112:1456-65.
38. Sviridov D, Hoang A, Ooi E, Watts G, Barrett PH, Nestel P. Indices of reverse cholesterol transport in subjects with metabolic syndrome after treatment with rosuvastatin. *Atherosclerosis* 2008;197:732-9.
39. Franceschini G, Calabresi L, Colombo C, Favari E, Bernini F, Sirtori CR. Effects of fenofibrate and simvastatin on HDL-related biomarkers in low-HDL patients. *Atherosclerosis* 2007;195:385-91.
40. Miyamoto-Sasaki M, Yasuda T, Monguchi T, et al. Pitavastatin increases HDL particles functionally preserved with cholesterol efflux capacity and antioxidative actions in dyslipidemic patients. *J Atheroscler Thromb* 2013;20:708-16.
41. Howe V, Chua NK, Stevenson J, Brown AJ. The regulatory domain of squalene monooxygenase contains a re-entrant loop and senses cholesterol via a conformational change. *J Biol Chem* 2015;290:27533-44.

42. Luu W, Zerenturk EJ, Kristiana I, Bucknall MP, Sharpe LJ, Brown AJ. Signaling regulates activity of DHCR24, the final enzyme in cholesterol synthesis. *J Lipid Res* 2014;55:410-20.
43. Wu BJ, Chen K, Shrestha S, Ong KL, Barter PJ, Rye KA. High-density lipoproteins inhibit vascular endothelial inflammation by increasing 3beta-hydroxysteroid-delta24 reductase expression and inducing heme oxygenase-1. *Circ Res* 2013;112:278-88.
44. Horton JD, Goldstein JL, Brown MS. SREBPs: activators of the complete program of cholesterol and fatty acid synthesis in the liver. *J Clin Invest* 2002;109:1125-31.
45. Voros S, Elashoff MR, Wingrove JA, Budoff MJ, Thomas GS, Rosenberg S. A peripheral blood gene expression score is associated with atherosclerotic plaque burden and stenosis by cardiovascular CT-angiography: results from the PREDICT and COMPASS studies. *Atherosclerosis* 2014;233:284-90.
46. Thomas GS, Voros S, McPherson JA, et al. A blood-based gene expression test for obstructive coronary artery disease tested in symptomatic nondiabetic patients referred for myocardial perfusion imaging the COMPASS study. *Circ Cardiovasc Genet* 2013;6:154-62.
47. Dudley JT, Tibshirani R, Deshpande T, Butte AJ. Disease signatures are robust across tissues and experiments. *Mol Syst Biol* 2009;5:307.
48. Kidd BA, Readhead BP, Eden C, Parekh S, Dudley JT. Integrative network modeling approaches to personalized cancer medicine. *Per Med* 2015;12:245-57.
49. Masud R, Shameer K, Dhar A, Ding K, Kullo IJ. Gene expression profiling of peripheral blood mononuclear cells in the setting of peripheral arterial disease. *J Clin Bioinforma* 2012;2:6.
50. Gautier EL, Ivanov S, Lesnik P, Randolph GJ. Local apoptosis mediates clearance of macrophages from resolving inflammation in mice. *Blood* 2013;122:2714-22.
51. Bartels ED, Christoffersen C, Lindholm MW, Nielsen LB. Altered metabolism of LDL in the arterial wall precedes atherosclerosis regression. *Circ Res* 2015;117:933-42.
52. Vengrenyuk Y, Nishi H, Long X, et al. Cholesterol loading reprograms the microRNA-143/145-myocardin axis to convert aortic smooth muscle cells to a dysfunctional macrophage-like phenotype. *Arterioscler Thromb Vasc Biol* 2015;35:535-46.

KEY WORDS fibrous cap thickness, high-dose statin, optical coherence tomography, plaque stability, thin-cap fibroatheroma

APPENDIX For an expanded Methods section as well as figures and tables, please see the online version of this article.